Experimental access to femtosecond spin dynamics

2003 J. Phys.: Condens. Matter 15 S723

(http://iopscience.iop.org/0953-8984/15/5/324)

INSTITUTE OF PHYSICS PUBLISHING JOURNAL OF PHYSICS: CONDENSED MATTER

J. Phys.: Condens. Matter **15** (2003) S723–S736 PII: S0953-8984(03)55594-1

Experimental access to femtosecond spin dynamics

B Koopmans, M van Kampen and W J M de Jonge

Center for NanoMaterials (cNM) and COBRA Research Institute, Department of Applied Physics, Eindhoven University of Technology, PO Box 513, 5600 MB, Eindhoven, The Netherlands

Received 5 November 2002
Published 27 January 2003
Online at stacks.iop.org/JPhysCM/15/S723

Abstract

In this paper we discuss various contributions to the transient magneto-optical (MO) response of ferromagnetic metals after laser-heating by a femtosecond pump pulse. It is demonstrated that a simple relation between MO response and the fast magnetization dynamics does not hold. A more general concept is introduced, on the basis of which artifacts are experimentally identified. Special focus is on problems associated with conservation of angular momentum in the ultrafast regime. A model describing dichroic state filling effects, fully including the coherent interactions between pump and probe pulses, is worked out. One of the potential methods to achieve access to the genuine magnetization dynamics, based on a thermal difference scheme, is analysed in detail. Finally, it is discussed how the different dynamical processes triggered by the laser pulse appear in the transient MO signal.

(Some figures in this article are in colour only in the electronic version)

1. Introduction

The dynamics of spin systems at a femtosecond timescale is an exciting issue that has received a growing interest over the past few years [1–6]. Although partly driven by the quest for information storage devices with an increasing capacity and speed, the field particularly addresses fundamental questions about the ultimate magnetic timescales. In this work we focus on one of the most intriguing ones: what is the timescale of the magnetic response after laser-heating of a ferromagnetic material by a femtosecond laser pulse? Two approaches to experimentally address this issue have been reported, time-resolved photoemission [6], and all-optical approaches with 'pump' and 'probe' laser pulses [1–5]. In this paper we predominantly focus on the latter approach.

The general layout for an all-optical approach to investigate the laser-induced demagnetization is schematically illustrated in figure 1. An intense laser pulse is used to heat up a ferromagnetic material. The temporal evolution of the magnetization, characterized by a transient magnetization $\vec{M}(t)$, is measured by recording the magneto-optical (MO) Kerr rotation $\tilde{\theta}(t)$ as a function of pump–probe delay time. The technique is generally denoted as TRMOKE (time-resolved magneto-optical Kerr effect).

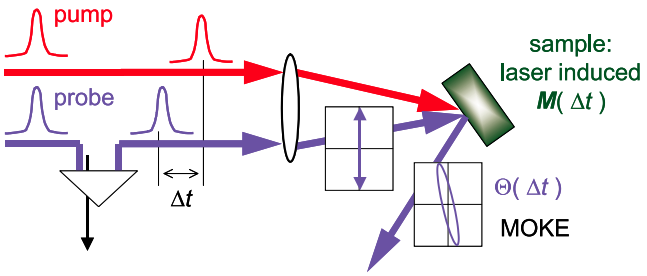

Figure 1. Schematic illustration of a TRMOKE set-up. A femtosecond pump pulse is focused on a ferromagnetic material, heating up the spin system. A second, time-delayed and linearly polarized, probe pulse is focused to an overlapping spot. Measuring the induced MO Kerr rotation as a function of the pump–probe delay (Δt) provides information on the evolution of the magnetic state.

Upon laser-excitation electron–hole pairs (hot electrons) are instantaneously generated. The hot electron gas rapidly thermalizes, after which its temperature (electron temperature) equilibrates with the lattice (indicated by a phonon temperature) within a timescale of approximately 1 ps for the metallic systems considered in the present work. Finally, it is known that once the spin system has come to equilibrium with electrons and lattice, it should be characterized by a reduced magnetization, due to the additional thermal disorder in the spin system. The central questions in the field of laser-induced femtosecond demagnetization are

(i) what is the timescale at which the equilibration (and thus demagnetization) of the spin system takes place, and
(ii) what are the processes involved?

By the mid-1990s it was generally believed that the demagnetization time τ_M was of the order of 100 ps [7, 8], and driven by the spin–lattice relaxation [9].

In this respect, pioneering experiments by Beaurepaire *et al* in 1996 [1] came as a big surprise to the scientific community. In their TRMOKE investigations on ferromagnetic thin films of nickel they found a loss of the MO contrast of several tens of per cent within the first picosecond. Later experiments by several groups reproduced the results [2, 4–6]. Even more strikingly, it was found that in many cases the loss in MO contrast was just limited by the width of the laser pulses used [10]. In fact, after deconvolution of the results this means a vanishingly small characteristic timescale, that is $\tau_M = 0$, within an experimental uncertainty of approximately 10 fs. As a consequence, the magnetization would be described by a direct (instantaneous) function of the electron temperature, $M(t) = M[T_e(t)]$.

These conclusions, however, are fully based on the existence of a direct relation between the MO response and the magnetization,

$$\tilde{\theta}(t) = FM(t). \tag{1}$$

The effective Fresnel coefficient F depends on details of the optical configuration, such as angle of incidence, laser wavelength, polarization, film thickness, choice of substrate etc, but is assumed to be a constant throughout the relevant timescales.

In this paper we will first (section 2) argue that an instantaneous demagnetization is quite unlikely, and replace equation (1) by a more general relation. In section 3 we discuss experimental results that have helped to identify some of the 'artifacts' that lead to a violation of equation (1). A potential scheme to access the 'genuine' magnetization dynamics is proposed in section 4. The resulting magnetic and nonmagnetic timescales derived this way for nickel will be briefly discussed in section 5, where some general mechanisms and their influence on

the MO response will also be introduced. Finally, a brief summary and a future outlook are presented in section 6.

2. Analysis of the problem

One of the most prominent and intuitive objections against an instantaneous laser-induced demagnetization is the constraint of the conservation of angular momentum. The spin and orbital moment of the electronic system are related to its magnetic moment

$$\vec{\mu} = \mu_B(\vec{L}_e + g\vec{S}_e), \tag{2}$$

where the g-factor is close to two for the materials considered here. In addition, these electronic moments are related to the total angular momentum of the system by

$$\vec{J} = \vec{L}_e + \vec{S}_e + \vec{L}_{phonon} + \vec{L}_{photon}. \tag{3}$$

Also included are a lattice (phonon) contribution to $\vec{J}$, as well as a contribution associated with the laser field (photons). Since the total Hamiltonian of the system conserves the total angular momentum, a change in magnetization can only be achieved by exchange among the four contributions on the right-hand side of equation (3).

As to potential exchange channels for a (quasi)instantaneous demagnetization (let us say, within 10 fs) an exchange of angular momentum with the photon field would provide an allowed channel. In fact, the process always occurs if circularly polarized light is absorbed, or if linearly polarized light is absorbed in a dichroic medium. Zhang and Hübner [11] have developed a model of ultrafast demagnetization in ferromagnetic nickel based on this principle. It should be realized, however, that the total amount of angular momentum transfer is limited by the number of photons involved in the laser field. Each photon can provide at most a single quantum of angular momentum. A simple estimate can than be made to check whether, potentially, photons play a significant role in current demagnetization experiments.

As a typical example we consider recent data of [5] for ferromagnetic nickel in an epitaxial Cu/Ni 13 nm/Cu structure. At a pulse energy of 1.6 nJ, focused down to a 10 μm diameter spot, a demagnetization by 5% was found, in good agreement with other reports. The loss of magnetic moment corresponds to 0.03 μ_B/atom. Based on the laser parameters, and having estimated an absorption of 20% of the incident light in the nickel film, it is easily found that $\approx$0.01 photon is absorbed per nickel atom. Although each photon could in principle contribute by a full μ_B, the small MO efficiency of the ferromagnetic transition metals—related to the quenching of the orbital momentum by crystal field effects—leads to a transfer of no more than 0.01 μ_B/photon. Altogether, photo-quenching of $\vec{M}$ is estimated to be not larger than 10^{-4} μ_B/atom, more than two orders of magnitude less then required to be of substantial relevance.

The possible role of phonons is nicely illustrated by a classical experiment by de Haas and Einstein in 1915 [13], demonstrating the concept of 'rotation by magnetization' [12]. A thin demagnetized ferromagnetic cylinder is connected to a thin fibre. After applying a sudden magnetic field along its main axis, the cylinder is magnetized. The induced magnetization will be compensated by a rotation of the body, i.e., an exchange occurs between S and L_{phonon}. Note that at the microscopic level, spin–orbit (SO) coupling is a necessary ingredient. Without its presence, there is no spin–lattice relaxation that converges the precessing motion of the electron spins towards a net magnetization parallel to the applied field. Returning to the laser-induced experiment, transfer of spin to lattice angular moment would allow for a fast demagnetization conserving the total J. In that case, the situation would be more or less the opposite of the de Haas–Einstein experiment; a net rotation of the irradiated area ('coherently

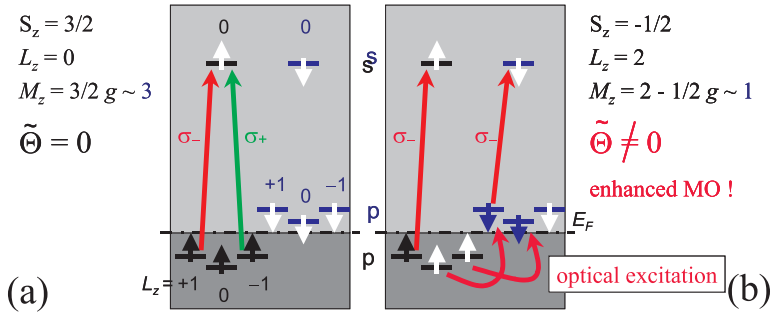

Figure 2. Simplified scheme of the influence of an SO-driven reduction of $\vec{M}$ on the MO response for an artifical p-electron ferromagnet. In the ground state (a) the spin-split p band is fully polarized, leading to a magnetic moment of $3/2g\mu_B \approx 3\ \mu_B$. The equal oscillator strength for + and − polarized light leads to a vanishing MO rotation, however. After two scattering processes in which J is conserved (b), the magnetic moment is reduced to $(2 - 1/2g)\mu_B \approx \mu_B$ though with a strongly enhanced MO response!

rotating phonons') would compensate the lost magnetic moment. However, it is generally believed that the phonon interactions are too slow to account for such a scheme occurring at a ∼10 fs timescale.

Having concluded that photons and phonons will be only of minor importance for a possible instantaneous effect, the explanation would rely on a fully electronic mechanism. Because of the conservation of $\vec{J}$, a reduction of $\vec{M}$ could only be achieved by an exchange of orbital and spin momentum in the electronic subsystem. This would lead, however, to rather peculiar—though challenging—effects. The (hypothetical) electronic configuration of figure 2 is used as a simple illustration. A p-type valence band is spin split in such a way that all minority levels are unoccupied. The only optical transitions included are those to an empty and spin-degenerate s level. The ground state is characterized by $S_z = 3/2$, $L_z = 0$ and $\mu_z = 3/2g\ \mu_B \approx 3\ \mu_B$. The MO response will be vanishingly small (if SO coupling is neglected), because of the cancelling contributions from the dipole-allowed transitions ($\Delta L = 0$) at opposite circular polarization, σ_+ and σ_-. Next we reconsider the system after a number of SO scattering events from majority to minority p states have occurred while conserving $\vec{J}$ ($J_z = 3/2$), as indicated in figure 2(b). After the scattering, in this specific case, we have $S_z = -1/2$, $L_z = 2$, and the magnetization is significantly reduced from $M_z = 3$ to $1\ \mu_B$. Despite this reduction of $\vec{M}$, the quenching of the transition at σ_+ and the newly available σ_- transition from the minority $L_z = +1$ state yield an enormous increase of MO response! Most clearly, the exchange of spin and orbital momentum gives rise to a severe violation of the simple relation between $\tilde{\theta}$ and M (equation (1)). This would actually mean that one is not allowed to conclude an instantaneous magnetic response ($\tilde{\theta}(t) = \theta(t) + i\epsilon(t)$, i.e. the sum of MO rotation and ellipticity) from the MO experiment!

The above analysis asks for the utmost care in drawing conclusions from the transient MO experiments. In a more general analysis, we should start from a generalized relation between the MO response and the magnetization dynamics,

$$\tilde{\theta}(t) = \mathcal{F}[M(t)]. \tag{4}$$

Without further proof, we neglect non-magnetic contributions to $\tilde{\theta}$ (which can generally be suppressed by utilizing appropriate experimental schemes [15]), and only consider one component of the magnetization (which is valid as long as $\vec{M}$ points along a fixed direction or the configuration is only sensitive to a single component). For materials considered here, it is

generally an accurate approximation to linearize equation (4),

$$\tilde{\theta}(t) = F(t)M(t), \tag{5}$$

i.e., the generalized Fresnel coefficient becomes explicitly time dependent. In a transient MO experiment, and assuming a weak perturbation limit, the induced MO response can be expanded to lowest order as

$$\Delta\tilde{\theta} = F_0\Delta M(t) + M_0\Delta F(t). \tag{6}$$

Here, laser-induced effects are denoted by Δ, and static (unperturbed) values by an index '0'. Most importantly, it is seen that in the transient MO response an explicit contribution from laser-induced Fresnel coefficients appears. Based on the severe distortion of the electronic material by the femtosecond laser excitation, inclusion of such an explicit dependence is required for a proper description of the ultrafast experiments.

3. Magneto-optical artifacts

If the direct relation between $\tilde{\theta}$ and M according to equation (1) were to hold, the following equality should be valid independent of delay time t:

$$\frac{\Delta\theta(t)}{\theta_0} = \frac{\Delta\epsilon(t)}{\epsilon_0} = \frac{\Delta M(t)}{M_0}, \tag{7}$$

i.e., temporal profiles of both MO channels equal that of the magnetization. As a consequence,

> any violation of equation (7) is direct and unambiguous evidence that the effective Fresnel factor has an explicit time dependence, and that the MO experiment does not directly reflect the magnetization dynamics.

In fact, this theorem can be generalized to any optical channel that is supposed to directly measure the magnetization,

$$\frac{\psi(t)}{\psi_0} = \frac{\Delta M(t)}{M_0}, \tag{8}$$

for any parameter $\psi(t)$ related to the magnetization via $\psi(t) = FM(t)$.

Over the past few years a number of experiments have been presented that demonstrated the necessity to include $F(t)$.

(1) Koopmans *et al* performed TRMOKE on Ni(111)/Cu/Ni epitaxial films [5], and found a significant deviation between $\Delta\epsilon(t)/\epsilon_0$ and $\Delta\theta(t)/\theta_0$ over the first 400 fs after laser excitation. Small, though significant deviations survived over ∼1.5 ps, after which a full convergence was achieved for all longer timescales, including precessive effects in the hundreds of picoseconds regime.

(2) Regensburger *et al* [4] showed that for some of the MO tensor components in time-resolved optical second-harmonic generation on a single-crystalline Ni(110) surface equation (8) was not valid. It was found that for a high enough laser fluence this particular signal $\psi(t)$ changed sign upon laser-heating, while it was carefully verified in a two-pump-pulse configuration that the magnetization did not reverse its orientation.

(3) Kampfrath *et al* [14] demonstrated in their TRMOKE experiments on iron thin films that the MO profile displayed profound differences when measured at different laser wavelengths (400 versus 800 nm).

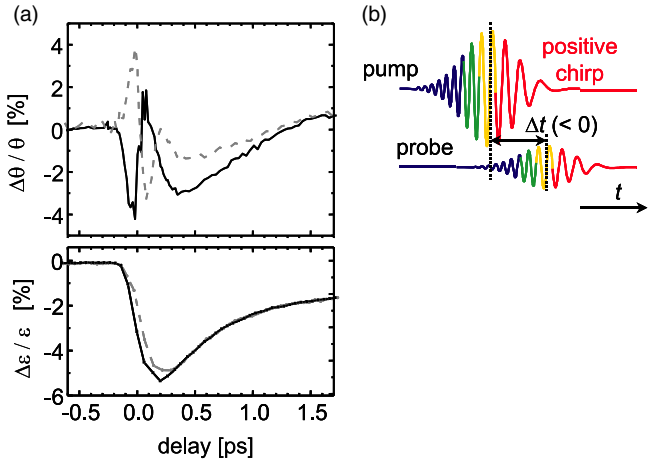

Figure 3. (a) Laser-induced rotation (top) and ellipticity (bottom) for negatively (solid black) and positively (dashed, grey) chirped pulses, as measured for an epitaxial nickel thin film. (b) Schematic illustration of the temporal profile of the pulses for a positive chirp ($b > 0$) and at a negative time delay.

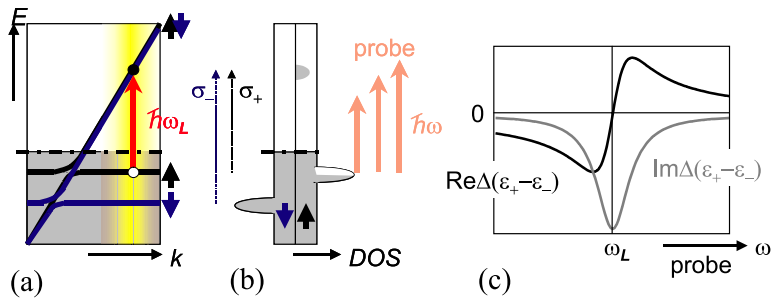

Figure 4. (a) Schematic band structure for a ferromagnetic transition metal, showing a dispersionless exchange-split d band, and a strongly dispersive though spin-degenerate sp band. The optical response is assumed to be dominated by the shaded area. (b) Redistribution of occupied states after laser excitation at frequency ω_L. (c) The resulting induced MO response, described by a Lorentzian, centred at $\omega = \omega_L$.

All of these experiments are unambiguous proofs that in the ultrafast regime a simple and direct relation between MO and magnetization does not always hold.

After having demonstrated their existence, it is one of the next tasks to identify mechanisms that contribute to the time dependence of F. A first experiment giving insight into the ultrafast regime is performing experiments with chirped laser pulses. Utilization of chirped pulses, in which different frequency components are delayed from one to the other, allows us to perform a two-colour experiment as illustrated in figure 3 [16]. The evolution of the TRMOKE signal on a Cu(001)/Ni/Cu sample was found to depend significantly on the magnitude and sign of the chirp. Whereas the ellipticity was relatively insensitive, the rotation showed a bipolar response around zero time delay, its overall phase reversing upon changing sign of the chirp. This behaviour can easily be explained by dichroic bleaching of the nickel film upon laser excitation, i.e., reducing the oscillator strength of MO transitions by state filling of high energy electronic levels [5, 17].

Right after laser-excitation—before any relaxation has set in—electronic states above the Fermi level have become occupied, whereas some of the previously occupied states below E_F have become empty. For a ferromagnetic material with exchange-split bands, this 'state filling' is intrinsically nonequivalent for the two spin bands. In the simplified case of figure 4, somewhat illustrative for ferromagnetic transition metals, it is assumed that upon laser excitation at frequency ω_L only transitions from the minority d band to the spin-degenerate sp band occur. As a consequence, probe photons will 'see' a perturbed electronic occupancy, and some transitions from the minority band are no longer allowed. In the presence of SO coupling this leads to a 'dichroic bleaching' of the material, described by a dip in the induced imaginary part of the off-diagonal dielectric response, $\Delta(\epsilon_+ - \epsilon_-) < 0$, peaked at a probe laser frequency ω equal to the pump frequency, $\omega = \omega_L$. The real part of the MO response is related via the Kramers–Kronig relations, i.e., changing sign right at ω_L. As a consequence, probing at a frequency just above the pump laser results in a positive real response, which is the case for a positive delay and at a negative chirp. Reversing the sign of the delay, or the sign of the chirp, leads to a reversal of the real response. In contrast, the imaginary response is expected to be relatively insensitive, and to transform even under reversal of chirp and delay time. The observed behaviour perfectly matches the predicted behaviour.

It could be argued, however, that the model described above is not a realistic one, since it fully neglects the coherence between the excited electron–hole pairs and the probe pulse. In fact, such a coherency should be included as long as pump and probe pulses have a temporal overlap, and can be incorporated within the density matrix formalism [18]. A distribution of electronic oscillators with homogeneous frequency distribution is assumed that is populated by a pump laser pulse. The successive relaxation of the electronic system is described by a Hamiltonian

$$H = H_0 + H_{pump} + H_{probe} + H_{random}, \tag{9}$$

where H_0 describes the unperturbed electronic system, the second and third term define the interaction with the pump and probe pulses, respectively, and the last term describes the randomizing interaction with an external heat bath. The system's evolution is described by the elements of the density matrix ρ_{ij}, where diagonal elements ($i = j$) represent the occupation of level i, and the off-diagonal elements ($i \neq j$) represent a coherent mixture of two states i and j. The coherent propagation of the system is calculated from [18]

$$\frac{\mathrm{d}\rho}{\mathrm{d}t} = [(H_0 + H_{pump} + H_{probe}), \rho]. \tag{10}$$

In addition, relaxation times T_1 and T_2 are defined to account for the population decay of diagonal elements, and the dephasing of off-diagonal elements of the density matrix, respectively. Finally, realistic laser pulses with a Gaussian profile, temporal width τ_L, central frequency ω_L, band width b_L and group-velocity dispersion parameter b are introduced, equal for pump and probe, though with a variable delay time Δt. Pump and probe pulses are assumed to be incident at different angles, such that the probe response can be truly separated from the reflected pump.

The results of the model for parameters fairly characteristic for transition metals ($T_1 =$ 20 fs, $T_2 = 10$ fs) are displayed in figure 5. In panel (a), the bleaching of a single oscillator is illustrated, whereas panel (b) displays the time-resolved bleaching for a dense set of oscillators. The antisymmetric response of the real part and the symmetric part of the imaginary part of the probe response as a function of delay time are clearly resolved. Most importantly, the sign of the real response reverses upon reversal of the group velocity dispersion b, exactly as observed in the experiment. Altogether, the fully coherent calculation reproduces qualitatively the features predicted by the hand-waving and intuitive incoherent approach. From the agreement of both

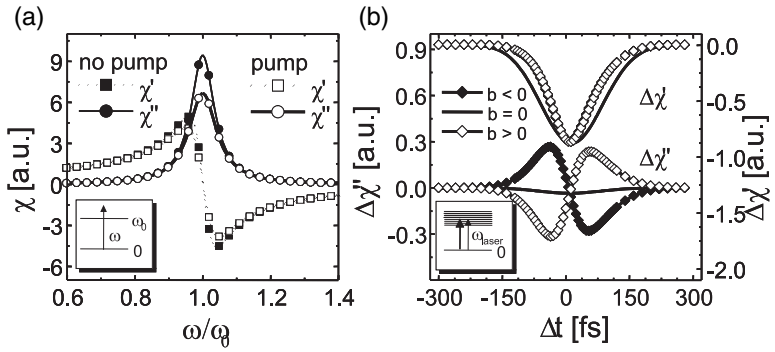

Figure 5. (a) Bleaching of a single oscillator at frequency ω_0, calculated within the density matrix formalism as explained in the text. The filled symbols represent the optical spectrum without pump pulse (expressed in terms of the real and imaginary parts of the susceptibility), the open symbols after switching the pump pulses on. (b) Transient optical response (represented by the pump-induced susceptibility $\Delta\chi$) with chirped pump and probe laser pulses, for a continuous distribution of harmonic oscillators, and calculated for different values of the chirp parameter b. Reversing b yields an inversion of the real response, while a similar reversal is observed as a function of delay time.

models with experiments we conclude that state filling effects play an important role in the transient contributions of the Fresnel coefficient F during the first few hundred femtoseconds.

Nevertheless, other artifacts may be of importance as well. In fact, evidence for a time dependence of F that lasts for tens to hundreds of *pico*seconds has been reported. As an example, in the experiment by Kampfrath *et al* the contrasting MO behaviour for different laser wavelengths (400 versus 800 nm) lasted for up to 100 ps. Van Kampen *et al* reported on a difference in induced rotation and ellipticity for an epitaxial nickel thin film on a (001)-cut Cu crystal, as shown in figure 6. In this specific case, and in sharp contrast with the (111) oriented film, deviations persist for tens of picoseconds, which most surely cannot be accounted for by electronic state filling effects. As an alternative mechanism, it is proposed that the uniaxial strain built up in the thin film upon laser-heating may effectively modify the MO response by a modification of the electronic band structure and MO anisotropy. Most importantly, it is seen that for the oscillatory signals in the MO response observable after hundreds of picoseconds a full agreement between rotation and ellipticity is observed, ruling out an erroneous calibration of one of the two complementary channels. In passing, we want to mention that the oscillatory signals have been attributed to a laser-induced precession of the magnetization vector [19].

To this end, we have discussed the occurrence of various contributions to the transient MO response after laser heating:

(1) dichroic bleaching, for which conclusive experimental evidence has been presented,
(2) MO strain effects, conjectured to be a possible explanation for long time effects, and
(3) exchange between orbital and spin-momentum, introduced in the previous section as a mechanism that most surely would lead to a nonequivalence of MO response and magnetization, though no experimental evidence has been reported for it so far.

4. Separation of the magnetization dynamics

After having read the previous section, the reader may have become a bit disappointed. Although much evidence for a really fast demagnetization has been gathered, the presence

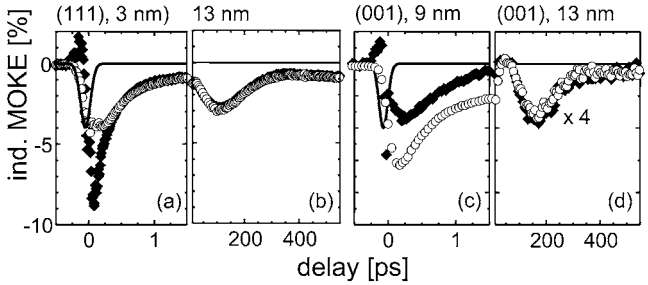

Figure 6. Transient MOKE on Cu/Ni/Cu epitaxial films, for a (111) (left) and (001) (right) orientation, and a thickness of the nickel layer as indicated. The full line represents the pump–probe autocorrelation profile. Differences between the induced rotation (filled symbols) and ellipticity (open symbols) vanish after 1–2 ps for the (111) case, while they persist for tens of picoseconds in the (001) case.

of the MO artifacts seems not to tolerate a serious estimate of the genuine magnetic timescale. Clearly we are hindered by our indirect optical view on the matter. A special scheme would be needed that discriminates between the artifacts and the magnetization dynamics.

A potential solution is obtained after realizing the different temperature dependence of truly magnetic and state-filling effects, represented by the two contributions in equation (6). The state filling effect, represented by $\Delta F(t)$, is expected to be only weakly sensitive to a few millielectronvolts additional thermal broadening. In sharp contrast, the induced magnetization dynamics is anticipated to be strongly temperature dependent. The higher T, and the closer to the Curie temperature, the more pronounced the effect of heating by an identical temperature interval ΔT will be. Formally, this dependence is described by

$$\frac{\Delta\theta(t)}{\theta_0} = \frac{\Delta F(t)}{F_0} + \frac{\Delta T_s(t)}{M_0}\frac{\mathrm{d}M(T)}{\mathrm{d}T}, \tag{11}$$

where $\mathrm{d}M/\mathrm{d}T$ represents the derivative of the equilibrium $M(T)$, and we have introduced an induced spin temperature $\Delta T_s(t)$. If any explicit temperature dependence of the heat capacities and thermal conductivities of the system can be neglected, a measurement of laser-induced MO dynamics at two different temperatures T_1 and T_2 will serve to achieve a final separation. In that case, the 'thermal difference' of the MO response will be completely dominated by the second term in equation (11),

$$\left.\frac{\Delta\theta(t)}{\theta_0}\right|_{T_2} - \left.\frac{\Delta\theta(t)}{\theta_0}\right|_{T_1} = \left(\left.\frac{1}{M_0}\frac{\mathrm{d}M(T)}{\mathrm{d}T}\right|_{T_2} - \left.\frac{1}{M_0}\frac{\mathrm{d}M(T)}{\mathrm{d}T}\right|_{T_1}\right)\Delta T_s(t). \tag{12}$$

The feasibility of this approach is demonstrated by the collection of results displayed in figure 7. First of all it is demonstrated that a significant dependence of the induced MO response on ambient temperature is indeed observed (figure 7(a)). Curves obtained for an epitaxial Ni(001) film at 373 K show a pronounced enhancement over data measured at 307 K, as expected from the steeper slope of $M(T)$ and the decrease of $1/M_0$ at elevated temperature. In passing we emphasize that the initial decrease of the MO ellipticity around zero time delay is quasi-instantaneous, i.e., just limited by the width of the laser pulse and well described by a time-integrated absorption profile.

Second, the difference of the results at the two contrasting temperatures is plotted, and compared to that of the rotation channel (figure 7(b)). Most strikingly, although the two complementary channels display a pronouncedly different behaviour when measured at a fixed temperature (see e.g. figure 6, rightmost two panels), the thermal difference signals completely

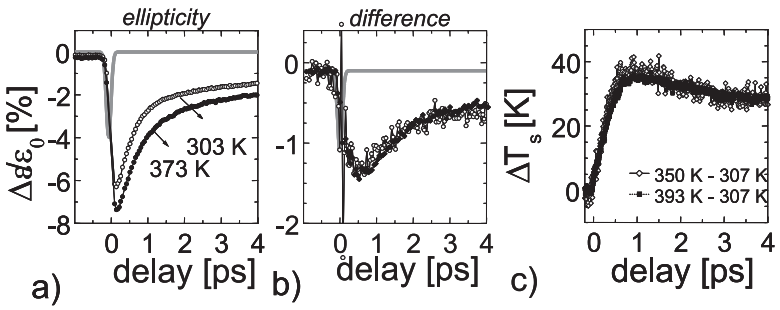

Figure 7. (a) Transient MO ellipticity at two ambient temperatures, showing the increased response at elevated T. The grey curve represents the pump laser profile. Data are obtained from an epitaxial Cu(001)/Ni/Cu film. (b) The corresponding thermal difference curves for ellipticity (filled) and rotation (open) completely overlap, and lack an instantaneous response at $t = 0$. (c) A similar experiment for a polycrystalline nickel film on an insulating buffer layer. Plotted is the spin temperature derived from the thermal difference MO response obtained over a small (open) and large (filled) temperature interval.

overlap within the experimental accuracy. Moreover, the instantaneous response is entirely absent. Rather, a gentle increase is observed, with a slope described by a time constant of a few hundred femtoseconds.

In order to verify the stability of the method, and to check whether the outcome depends on the temperature interval chosen figure 7(c) displays the analysis for a polycrystalline Ni film on a thermally insulating Si_3N_4 layer, but now measured at a larger number of temperatures. The much slower recovery in this case as compared to the nickel films directly on copper might be due to the slower heat diffusion. Most importantly, it is shown that halving the temperature interval over which the thermal difference scheme is applied does not alter the outcome within the experimental accuracy. This provides experimental evidence for the minor role of temperature-dependent diffusion effects. Moreover, it shows that the resolved magnetic timescale is relatively temperature independent, and characteristic for at least a temperature range between 300 and 400 K.

Other checks on different materials have been performed, including ultrathin ($<$1 nm) Co layers sandwiched between two Co films. Based on experience with this multitude of systems, it is concluded that the method is quite generally applicable. However, the analysis becomes nontrivial when approaching the Curie temperature too closely, because of the contribution of nonlinear terms, that is, when going beyond the weak perturbation limit. Moreover, a relatively small, though reproducible dependence of the transient response on laser fluence has been found. At this stage it is not completely clear whether those effects have to be attributed to a slight temperature dependence of diffusion, or rather to a dependence of the relaxation channels on excitation density. In addition, we recently found that the temperature dependence of the electronic specific heat might have to be included in order to come to a fully quantitative interpretation of the thermal difference scheme. More research is obviously needed to draw final conclusions.

Nevertheless, all results so far have reproduced an intrinsic demagnetization time of ferromagnetic nickel of 200–400 fs, slightly depending on the exact model utilized to extract the timescale. Within these limits, no significant dependence on extrinsic parameters, such as film thickness and morphology of the film, has been found. Thus, the reported value is believed to be the intrinsic magnetic timescale for nickel. Independent of the detailed interpretation, however, an instantaneous magnetic respons has been definitely ruled out.

5. Discussion

The validity of the thermal difference scheme is based on several assumptions. In the forthcoming discussion, we first address the effect of a number of relaxation mechanisms on the transient MO response, in order to assess the validity of the thermal difference scheme in some more detail. Then, we will compare the magnetic timescale derived in the previous section to that of electron–phonon relaxation, after which the potential role of phonons in the ultrafast demagnetization will be discussed.

Excitation by a short laser pulse triggers a number of processes, each of which affects the (magneto-) optical response in a different way.

(1) Upon interaction with the pump laser pulse, electrons are excited with an energy of the order of an electronvolt above the Fermi level. The strong perturbation of electronic occupation gives rise to an immediate change in both diagonal and off-diagonal optical responses, and is the origin of the 'dichroic bleaching', fully described by the ΔF term in equation (6).
(2) Within a thermalization time of at most a few hundred femtoseconds, the hot electrons relax to a thermal equilibrium. In the thermalized situation the redistribution of occupied electronic states is limited to states near the Fermi level. Assuming that those states are 'probed' in a nonresonant way, it is easily derived that the transient reflection scales linearly with the excess energy in the electron system in this regime [20]. Similarly, a certain contribution from the thermal electrons to the MO response cannot be excluded without a more thorough analysis. The *phase* of the induced dielectric tensor element $\Delta\epsilon_{xy}$ in this non-resonant regime is unrelated to that right after excitation.
(3) The successive equilibration of electrons and lattice is mediated by electron–phonon scattering and characterized by the energy relaxation time τ_E. The modified band structure, and the reduction of the electron density of the lattice after its uniaxial expansion, affect the optical response as well. At longer timescales, a shock wave may develop and bounce back and forth in thin film media, accompanied by a periodically perturbed optical response. The MO strain effect, introduced in section 3, can be considered as the MO analogue of the lattice contribution to the transient reflection, and is fully accounted for by a 'long' timescale contribution to ΔF.

While mechanisms 1–3 affect the magnetic and nonmagnetic response on a more or less equal footing, the final loss of magnetic order has its main effect on the MO channel. We can identify two potential mechanisms.

(1) In the first scenario, long wavelength spin fluctuations are considered that do not alter the local magnetic moment. Thus, the exchange splitting is assumed constant up to the Curie temperature. The demagnetization is just treated as a spatial disorder in the quantization access. As a consequence, the only effect of the demagnetization on $\Delta\tilde{\theta}$ is via ΔM. This view is supported, e.g., by the observation by spin-resolved photoemission of local moments even above T_c [21].
(2) Alternatively, we can treat the demagnetization in the opposite limit, assuming that the exchange splitting in the energy bands scales directly with the magnetic moment $M(T)$, and thus continuously vanishes while approaching T_c. In this approach, supported, e.g., by angle-resolved photoemission studies [22], $\Delta\theta/\theta_0$ would be no longer solely equivalent to $\Delta M/M_0$. Due to the altered band structure accompanying the modified exchange splitting, contributions are introduced that are similar to state filling. The phase and amplitude of such a signal will strongly depend on details of the band structure and frequency of the probe laser.

The last scenario is obviously the most difficult to treat. One may wonder about the impact on the interpretation of some of the experiments, discussed in preceding sections. The fact that the phase of $\Delta\tilde{\theta}$ is not equal to that of $\tilde{\theta}$ means that the normalized transient MO rotation and ellipticity would no longer necessarily overlap. Thus, the observation of a fast convergence of MO rotation and ellipticity may be considered as an indication of minor contributions from a transient exchange splitting.

Despite the more complex relation between M and $\tilde{\theta}$, within the weak perturbation approach one may assume $\Delta\theta \propto \Delta M$ even under scenario 2. Thus, one would expect the same temporal dependence (though different amplitudes) for the two complementary channels, i.e., $\Delta\theta(t)/\Delta\epsilon(t)$ is constant. We conclude that, independent of which of the two descriptions of the demagnetization is being adapted, the thermal modulation would provide the genuine magnetization dynamics.

Another point of concern is the diffusion of heat from the heated layer. Since the absorption depth of the laser light is typically only 10–15 nm, and thermal diffusion over distances of nanometres in metals proceeds within picoseconds, such nonlocal effects cannot be excluded *a priori*. If included, a potential temperature dependence of the diffusion constants may provide an erroneous source of thermal difference in $\Delta\theta/\theta_0$. In the examples discussed in the preceding section, it was carefully verified that these effects were found to be negligible at least for the fast dynamics observed over the first picosecond [5]. Such a check needs to be made explicitly, however, whenever applying the thermal difference schemes. We emphasize that details in thermal difference curves after picoseconds may well be driven by a subtle thermal dependence of the diffusive dynamics.

Finally, in deriving equation (12) we explicitly assumed the heat capacitance of the electron and lattice system to be independent of temperature. It can be shown, however, that in the more general case the temporal profile of the spin temperature is not necessarily equal at both temperatures. In that case, a generalized and more complicated approach may be required, which is a matter of current investigation.

After discussing the effects of various mechanisms on the MO response, and providing a further validation of the thermal difference scheme, it is worthwhile to discuss its resulting demagnetization time of 0.2–0.4 ps for ferromagnetic nickel. A particular interesting observation has been its close resemblance to the e–p relaxation. Transient reflectance studies on nickel have resulted in τ_E of only a few tenths of a picosecond, that is, rather close to τ_M. This observation might imply a potential role of phonons in the demagnetization process, somewhat related to the ordinary spin–lattice relaxation, though occurring at the sub-picosecond domain. While such a mechanism would solve the problems associated with conservation of angular momentum, the lattice providing a source of J, no serious models accounting for such a phonon-driven ultrafast demagnetization have been reported yet.

In order to check whether phonons may play a role at all, we can make an estimate along the lines of section 2. In the example of the Cu/Ni 13 nm/Cu structure at a pulse energy of 1.6 nJ, an excitation density of 0.01 was found [5]. Using a photon energy of approximately 1.6 eV, yields a deposited energy of 16 meV/atom. Realizing that the energy of zone edge phonons is 40 meV leads to a minimum of 0.4 e–p scattering events per atom during the first few hundred femtoseconds. Similarly, in the same time the magnetic moment per nickel atom is reduced by 0.03 μ_B, which requires at least 0.03 spin-flip events per nickel atom. Altogether, demagnetization by phonons would suffice, if approximately a fraction of $0.03/0.4 \sim 0.07$ of the e–p scattering processes were to be accompanied by a spin-flip event. This number could be interpreted as an Eliot–Yafet parameter for hot electrons in ferromagnetic transition metals [23]. A theory for these materials under the extreme conditions of laser excitation is not available. Nevertheless, the thermal equilibrium values for noble metals known to range

from $\sim$0.001 for the 3d elements to $>$0.1 for gold may be thought of as a motivation to further explore this route.

6. Conclusions and outlook

The main theme of this paper was the analysis of laser-induced femtosecond demagnetization experiments. The occurrence of an instantaneous demagnetization was shown to be in conflict with conservation of angular momentum, once a simple interpretation of the MO experiment is adapted. A more general framework, describing the transient MO response as a sum of contributions scaling directly with the induced magnetic moment (ΔM), and with transient effects in the effective Fresnel coefficient (ΔF), respectively, was introduced.

The absence of a direct relation between the magnetization dynamics and the transient MO response was demonstrated by discussing a number of recent experiments. Some 'artifacts' could be unambiguously identified. Experiments with chirped laser pulses resolved the contribution of state-filling effects, a phenomenon denoted 'dichroic bleaching'. Nonmagnetic ('ΔF') contributions to the MO response persisting to tens of picoseconds were tentatively attributed to MO strain effects.

A thermal difference scheme for accessing the genuine magnetization dynamics was introduced. Its experimental soundness was demonstrated in a number of experiments on different nickel- and cobalt-based systems. The validity of some of the basis assumptions was addressed by discussing several relaxation mechanisms. The close resemblance of the resulting demagnetization time (a few hundred femtoseconds for nickel) with the e–p equilibration time, led to the conjecture of a possible role of phonons in the femtosecond demagnetization process. A simple estimate indicated that a realistic fraction of 0.1 of the e–p scattering events should be accompanied by a spin flip.

Recent progress in ultrafast MO experiments has clearly identified some complications, but has also provided routes to a sound access of magnetization dynamics. The interpretation of the surprisingly fast magnetic response in terms of elementary mechanism is believed to be the next goal. Serious efforts, both in theory and experiment, will be needed to make further progress in this challenging field of research. Not only will these efforts contribute to our fundamental understanding of the ultimate limits of magnetization dynamics, also potential contributions to the field of spintronic devices and hybrid recording schemes may be anticipated.

References

[1] Beaurepaire E, Merle J-C, Daunois A and Bigot J-Y 1996 *Phys. Rev. Lett.* **76** 4250–3
[2] Hohlfeld J, Matthias E, Knorren R and Bennemann K H 1997 *Phys. Rev. Lett.* **78** 4861–4
[3] Beaurepaire E, Maret M, Halté V, Merle J-C, Daunois A and Bigot J-Y 1998 *Phys. Rev.* B **58** 12134–7
[4] Regensburger H, Vollmer R and Kirschner J 2000 *Phys. Rev.* B **61** 14716–19
[5] Koopmans B, van Kampen M, Kohlhepp J T and de Jonge W J M 2000 *Phys. Rev. Lett.* **85** 844–7
[6] Scholl A, Baumgarten L, Jacquemin R and Eberhardt W 1997 *Phys. Rev. Lett.* **79** 5146–9
[7] Vaterlaus A, Beutler T and Meier F 1991 *Phys. Rev. Lett.* **67** 3314–17
[8] Vaterlaus A, Beutler T, Guarisco D, Lutz M and Meier F 1992 *Phys. Rev.* B **46** 5280–6
[9] Hübner W and Bennemann K H 1996 *Phys. Rev.* B **53** 3422–7
[10] Güdde J, Conrad U, Jähnke V, Hohlfeld J and Matthias E 1999 *Phys. Rev.* B **59** R6608–11
[11] Zhang G P and Hübner W 1999 *Phys. Rev. Lett.* **85** 3025–8
[12] Richardson O W 1908 *Phys. Rev.* **26** 248–53
[13] Einstein A and de Haas W J 1915 *Verhandl. Deuts. Phys. Ges.* **17** 152
[14] Kampfrath T, Ulbrich R G, Leuenberger F, Münzenberg M, Sass B and Felsch W 2002 *Phys. Rev.* B **65** 104429-1–6
[15] Koopmans B, van Kampen M, Kohlhepp J T and de Jonge W J M 2000 *J. Appl. Phys.* **87** 5070–2

[16] van Kampen M, Koopmans B, Kohlhepp J T and de Jonge W J M 2002 unpublished
[17] Hübner W and Zhang G P 1998 *Phys. Rev.* B **58** R5920–R5923
[18] Yariv A 1989 *Quantum Electronics* (New York: Wiley)
[19] van Kampen M, Jozsa C, Kohlhepp J T, LeClair P, Lagae L, de Jonge W J M and Koopmans B 2002 *Phys. Rev. Lett.* **88** 227201
[20] Groeneveld R G H, Sprik R and Lagendijk A 1995 *Phys. Rev.* B **51** 11433
[21] Sinkovic B, Tjeng L H, Brookes N B, Goedkoop J B, Hesper R, Pellegrin E, de Groot F M F, Altieri S, Hulbert S L, Shekel E and Sawatzky G A 1997 *Phys. Rev. Lett.* **79** 3510–13
[22] Kreutz T J, Greber T, Aebi P and Osterwalder J 1998 *Phys. Rev.* B **58** 1300–17
[23] Yafet Y 1963 *g*-factors and spin–lattice relaxation times of conduction electrons *Solid State Physics* vol 14, ed F Seit and D Turnbull pp 1–98